Impact of the chemical composition of poly-substituted hydroxyapatite particles on the in vitro pro-inflammatory response of macrophages

Nathalie Douard, Lara Leclerc, Gwendoline Sarry, Valérie Bin, David Marchat, Valérie Forest, Jérémie Pourchez

Impact of the chemical composition of poly-substituted hydroxyapatite particles on the *in vitro* pro-inflammatory response of macrophages

Nathalie Douard[1,2] *, Lara Leclerc[2,3,4], Gwendoline Sarry[2,3,4], Valérie Bin[2,4,5], David Marchat[1,2], Valérie Forest[2,3,4], Jérémie Pourchez[2,3,4]

[1] Ecole Nationale Supérieure des Mines, CIS-EMSE, CNRS:UMR 5307, 158 cours Fauriel, F42023, Saint-Etienne, FR

[2] SFR IFRESIS, Saint-Etienne, FR

[3] Ecole Nationale Supérieure des Mines, CIS-EMSE, 158 cours Fauriel, F42023, Saint-Etienne, FR

[4] LINA EA4624, Laboratoire Interdisciplinaire d'Etude des Nanoparticules Aérosolisées, Université Jean Monnet, 10 rue de la Marandière, 42270, Saint-Priest en Jarez, FR

[5] Faculté de Médecine Jacques Lisfranc, Université Jean Monnet, 10 rue de la Marandière, 42270, Saint-Priest en Jarez, FR

*Correspondence should be addressed to: Nathalie Douard

Email: douard@emse.fr

Telephone number: +33 4 77 42 01 21

Fax number: +33 4 77 49 96 94

Abstract

To improve the biological properties of calcium phosphate (CaP) bone substitute, new chemical compositions are under development. *In vivo* such materials are subject to degradation that could lead to particles release and inflammatory reactions detrimental to the bone healing process. This study aimed at investigating the interactions between a murine macrophage cell line (RAW 264.7) and substituted hydroxyapatite particles presenting promising biological properties. Micron size particles of stoichiometric and substituted hydroxyapatites (CO_3 substitution for PO_4 and OH; SiO_4 substitution for PO_4; CO_3 and SiO_4 co-substitution) were obtained by aqueous precipitation followed by spray drying. Cells, incubated with four doses of particles ranging from 15 to 120 µg/mL, revealed no significant LDH release or ROS production, indicating no apparent cytotoxicity and no oxidative stress. TNF-α production was independent of the chemistry of the particles; however the particles elicited a significant dose-dependent pro-inflammatory response. As micron size particles of these hydroxyapatites could be at the origin of inflammation, attention must be paid to the degradation

behavior of substituted hydroxyapatite bone substitute in order to limit, *in vivo*, the generation of particulate debris.

Keywords: substituted hydroxyapatite; macrophage; cytotoxicity; inflammation

Acknowledgments

The authors would like to thank Agathe Figarol and Andréa Kurtz-Chalot for their help regarding the biological evaluation of the particles. The authors wish to thank the IFRESIS (Institut Fédératif de Recherche en Sciences et Ingénierie de la Santé) for the financial support provided for this work.

1. Introduction

The number of patients undergoing surgical bone reconstruction after trauma, cancer or malformations significantly increases (Planell et al. 2009). Surgery procedures mainly involve the use of autografts, allografts or xenografts. However, these options suffer from many disadvantages like morbidity and limited availability for the autografts or risks of rejection for the allografts and the xenografts (Oryan et al. 2014). To bridge this gap and to meet these drawbacks, synthetic bone substitutes have been developed since the 80s. Among them, calcium phosphate (CaP) based materials, such as hydroxyapatite (HA) and beta-tricalcium phosphate (β-TCP), present a high chemical similarity with the mineral component of bone (Rey et al. 2009) as well as an excellent biocompatibility with human tissues (Dorozhkin et al. 2002). They have been implanted clinically for more than 30 years either in the form of porous block or granules to fill bone defect, but also as a coating of metallic part of prostheses to promote their osteointegration (Campana et al. 2014).

Following the implantation of HA or β-TCP biomaterial, biological and biochemical process occur at the implant-tissue interface, such as biomaterial degradation and release of ions, protein adsorption and cell adhesion. These key events, that govern the appositional bone growth and its quality, are affected by the physiological environment at the implantation site (*e.g.* perfusion, pH, loading) as well as by the intrinsic properties of the biomaterial such as its solubility, permeability or wettability (Bouet et al. 2015). The *in vivo* degradation of CaP based biomaterial results from cell-mediated resorption, through the generation of an acidic extracellular compartment surrounding the material, and from chemical dissolution in physiological medium (Detsch et al. 2008; Raynaud et al. 2002). *In vivo* studies have shown that particulate debris can be released during the degradation of CaP bioceramics (Benhayoune et al. 2000; Hing et al. 2007; Lu et al. 2004). In addition to destabilize the early bone apposition, these debris can cause adverse immunogenic responses

orchestrated by cells of the monocyte/macrophage lineage that impair the natural bone healing process (Hing et al. 2007; Lu et al. 2004). Once debris are phagocytosed, pro-inflammatory mediators are released including tumor necrosis factor-alpha (TNF-α), interleukin IL-1β and IL-6 (Curran et al. 2005; Lange et al. 2009; Lange et al. 2011; Laquerriere et al. 2003; Velard et al. 2013). As some of these cytokines are involved in the differentiation of the bone resorbing osteoclasts cells (Lange et al. 2009), they can impair the balance between bone formation and resorption. In this context, particles of CaP based materials, like HA, β-TCP or biphasic calcium phosphate, have been proved to elicit a pro-inflammatory response *in vivo* (Hing et al. 2007) and *in vitro* using various cell lines (Curran et al. 2005; Lange et al. 2009; Lange et al. 2011; Laquerriere et al. 2003; Ninomiya et al. 2001; Zhang et al. 2012).

Ideally, CaP bone graft materials should provide a framework for bone growth and be degraded only when the woven bone tissue became a mature bone tissue (Heljak et al. 2012). The ability of CaP materials to be degraded and to foster the bone ingrowth is highly dependent on their chemical composition. For instance, HA displays a low rate of biodegradation as compared to β-TCP that is highly soluble (Barralet et al. 2000; Detsch et al. 2008). Moreover, HA shows limited ability to stimulate the development of new bone tissue (Porter et al. 2005; Spence et al. 2010). Thus, the performances of currently available synthetic biomaterials (HA and β-TCP) are not fully optimal for regenerative medicine. To further improve their biological properties, ionic substitutions into the HA crystal lattice are investigated (Shepherd et al. 2012). Among the ionic groups of biological interest, carbonate and silicate appear to be promising candidates to improve the biological properties of HA.

Literature has reported the beneficial effect of carbonate substitution for phosphate and/or hydroxide in HA. *In vivo* data have shown the formation of higher amount of new and mature bone into porous implant of carbon-substituted hydroxyapatite (CHA) than into HA (Landi et al. 2003). Moreover, the incorporation of carbonate into HA increases its solubility (Barralet et al. 2000; Porter et al. 2005) and its osteoclastic resorption in a dose-dependent manner (Spence et al. 2010; Spence et al. 2009). In addition, it is well known that silicon plays an essential role in bone metabolism (Carlisle 1970; Carlisle 1972). At physiological levels, soluble silicon was found to enhance osteoblastic cells differentiation (Reffitt et al. 2003) and to increase the bone mineral density (Jugdaohsingh 2007). That is why silicon-substituted hydroxyapatite (SiHA) is expected to improve the bone growth rate and quality over HA and has been widely studied over the last few years (Marchat et al. 2013). Carbon- and silicon-substituted hydroxyapatite (CSiHA) could represent an interesting co-substitution. Indeed, this CO_3 and SiO_4 co-substitution into HA may result in a synergy between the CHA biodegradation properties and the release of soluble silicate. To date, very few studies deal with the elaboration and the biological

evaluation of CSiHA. However, Landi et al. (2010) have indicated that for low amount of silicon (0.55 wt.%), CSiHA is not toxic for human osteoblasts. Solubility of CSiHA is greater than that of HA samples and is accompanied "by silicon ions release" (Bang et al. 2014; Pavankumar 2011). Even though CHA, SiHA and CSiHA bioceramics appear biocompatible in their bulk form, a lack of knowledge remains concerning the effects of debris released through their degradation. Thus, the present study is a preliminary work whose aim is to investigate the *in vitro* toxicity and pro-inflammatory response of these hydroxyapatites particles by means of macrophage cell line. To avoid a potential size or shape effect, substituted hydroxyapatite particles with similar morphologies were prepared. To this aim, powders with well-controlled chemical composition were synthetized *via* a wet precipitation method and the particles were shaped by spray drying. Their physical properties were adjusted by means of specific thermal treatment depending on their chemical compositions. The biological responses they induce were then evaluated regarding several parameters: Lactate Dehydrogenase (LDH) release (reflecting the integrity of the cell membrane), Tumor Necrosis Factor alpha (TNF-α) production (to assess the inflammatory response) and the production of different Reactive Oxygen Species (ROS).

2. Material and methods

2.1. Chemical synthesis of substituted hydroxyapatite particles

Four types of particles differing by their chemistry were studied: hydroxyapatite (HA), carbon-substituted hydroxyapatite (CHA), silicon-substituted hydroxyapatite (SiHA) and carbon-silicon co-substituted hydroxyapatite (CSiHA). They were prepared according to the following theoretical formulas : $Ca_{10}(PO_4)_6(OH)_2$ for HA, $Ca_{10}(PO_4)_{5.6}(SiO_4)_{0.4}(OH)_{1.6}$ for SiHA, $Ca_{9.2}(PO_4)_{5.2}(CO_3)_{0.8}(OH)_{1.2}$ for CHA and $Ca_{9.6}(PO_4)_{4.8}(CO_3)_{0.8}(SiO_4)_{0.4}(OH)_{1.6}$ for CSiHA. The powders were synthesized through an aqueous precipitation method according to a protocol that has been developed for the synthesis of monophasic SiHA with controlled stoichiometry (Boyer et al. 2013; Marchat et al. 2013). Briefly, a diammonium hydrogen phosphate aqueous solution ($(NH_4)_2HPO_4$, 99%, Merck, Germany), and, if applicable, an ammonium hydrogen carbonate aqueous solution ($(NH_4)HCO_3$, 99%, Merck, Germany) and an alkaline silicate solution were added to a calcium nitrate aqueous solution ($Ca(NO_3)_2$, $4H_2O$, 99%, Merck, Germany) maintained under stirring. The reactions were performed under argon flow. The pH of the suspension was adjusted (at 9.5 for HA, 8.0 for CHA, 11.0 for SiHA and 10.8 for CSiHA) by the addition of a 28% ammonia solution (Merck, Germany) by means of a dosing pump (ProMinent, Germany) coupled with a pH controller and sensor. The temperature was regulated at 50°C for HA, SiHA and CSiHA and 65°C for CHA with an external T-probe connected to a cryothermostat (Huber, Germany).

Suspensions were matured for 24 h, centrifuged at 1500 rpm for 5 min (Thermo Scientific, France) to eliminate the excess of ammonia solution and resuspended in distilled water. The resulting suspensions were then spray dried (Büchi B290, Germany) and finally, a thermal treatment under a specific atmosphere, depending on the chemistry, was applied (Table 1).

2.2. Physico-chemical characterization of substituted hydroxyapatite particles

Crystalline phases were identified using a Siemens D5000 θ/2θ X-ray diffractometer using CuKα radiation. Diffractograms with a step size of 0.02° and a counting time of 9 s by step were acquired. Standard patterns from International Center for Diffraction Data – Powder Diffraction Files (ICDD-PDF) were used for phase identification. Fourier transform infrared (FTIR) spectroscopy measurements were carried using a MIR TF Vertex 70 Spectrometer by means of the ATR system. Collected spectra over the range 4000–400 cm^{-1} were normalized from the ν_4 band of the phosphate group at 600 cm^{-1} as usual (Rey et al. 1989).

The silicon contents were determined using Inductively Coupled Plasma Atomic Emission Spectrometry (ICP/AES) (Spectrometer HORIBA, Jobin-Yvon, with Activa model) after dissolution of the samples in nitric acid solution. The carbon contents were measured using an elemental analyzer with an infrared detector (Leco CS-444 carbon and sulfur analyzer). All these analyses were performed in triplicate.

Morphology of the particles were observed using Scanning Electron Microscopy (SEM JEOL 6500 F). Samples were prepared by dispersing the particles in absolute ethanol. After sonication at 40 W for 5 min (Branson Sonifier) a drop of the suspension was deposited on a carbon-coated film and sputtered with gold (Quorum, Q150RES, England). The specific surface areas (SSA) were determined by N_2 adsorption after out-gassing for 12 h at 110°C (Micromeritics ASAP 2020) using the Brunauer–Emmet–Teller (BET) 5 points method. The particle size range was analyzed by laser diffraction method (Mastersizer 2000, Malvern). A suspension of particles was prepared with a dispersant (Darvan® C, Vanderbilt Minerals) and then sonicated at 40 W for 5 min (Branson Sonifier) before analysis.

2.3. Cell culture and cells-particles contact

Prior to suspension preparation, the particles were treated at 210°C for 30 min to sterilize the samples and to avoid the presence of endotoxins that may result in measurement bias. The suspensions were prepared in culture medium: Dulbecco's modified Eagle's medium (DMEM, Invitrogen) complemented with 10% of fetal calf serum (FCS, Invitrogen), 1% penicillin-streptomycin (penicillin 10,000 U/mL, streptomycin 10 mg/mL; Sigma-Aldrich, France). Particle concentrations of 15, 30, 60 and 120 μg/mL were used for the toxicity assays. A stock

solution at 120 µg/mL was dispersed by sonication at 40 W for 5 min (Branson Sonifier) and then diluted to obtain the other particles concentrations. All the suspensions were kept at 4°C and used in the following 48 h.

Biological assays were carried out using the RAW 264.7 cell line, provided by ATCC Cell Biology Collection (Promochem LGC, France) and derived from mice peritoneal macrophages transformed by the Albeson Murine Leukemia Virus. Cells, seeded at 100,000 cells/well, were prepared in 96-well plates in 50 µL of complemented DMEM and were allowed to adhere overnight at 37°C in a 5% CO_2 humidified atmosphere. 150 µL of particles suspensions were added to the culture and incubated for 90 min or 24 h. A negative control was performed incubating cells alone (without particles).

2.4. Cellular morphology

Cells incubated with particles for 24 h were gently removed with a scraper, deposited on glass plates and cytocentrifuged for 10 min at 400 rpm (Cytospin Shandon). Samples were air dried over night at room temperature before a May Grunwald Giemsa staining (MGG). Optical images were acquired with Leica DM750.

2.5. Cellular membrane integrity

Cytotoxicity was evaluated by quantifying the Lactate Dehydrogenase (LDH) released in culture supernatant from cells with damaged membranes. After a 24 h incubation with particles, the CytoTox-96® Non-radioactive Cytotoxicity Assay (Promega) was used according to the manufacturer's instructions. To obtain the positive control, 20 µl of 10X lysis solution provided by the manufacturer was added 45 min before analysis. Detection was performed using a microplate reader (Multiskan GO, Thermo Scientific) at 490 nm. The activity of the released LDH was reported as a percentage of the total cellular LDH (measured after the lysis of control cells).

2.6. Pro-inflammatory response

After 24 h incubation with particles, Tumor Necrosis Factor alpha (TNF-α) production was assessed using a commercial ELISA kit (Quantikine® Mouse TNF-α Immunoassay, R&D systems) according to the manufacturer's instructions. The optical density of each well was determined using a microplate reader (Multiskan GO, Thermo Scientific) set to 450 nm. A standard curve was established and results were expressed in pg of TNF-α per mL of supernatant.

2.7. Oxidative stress

Oxidative stress was estimated by measuring the intracellular ROS level using the OxiSelect™ Intracellular ROS Assay Kit (Cell Biolabs) after 90 min (for acute oxidative stress evaluation) and 24 h incubation with the particles. The assay employs the conversion by ROS of a non-fluorescent substrate, 2',7'-Dichlorodihydrofluorescin diacetate (DCFH-DA), which can easily diffuse through cell membranes into a

molecule DCF (2', 7'-Dichlorodihydrofluorescein) which is highly fluorescent and amount of which is proportional to total ROS. A 1 h pre-treatment with the cell-permeant DCFH-DA was carried out before particles incubation. The fluorescence intensities were read at 480 nm excitation and 530 nm emission (Fluoroskan Ascent, Thermo scientific). Results were expressed in nM of DCF produced per hour.

2.8. Statistical analysis

Results were expressed as the mean of three independent experiments carried out in quadruplets, with standard errors of the mean value (SEM). Statistical significance was declared when $p<0.05$ using a Bonferroni post-test after a two-way ANOVA.

3. Results

3.1. Physico-chemical features of substituted hydroxyapatite particles

After thermal treatment (Table 1), the particles displayed only the crystalline phase matching the ICDD standard for hydroxyapatite (HA, PDF 9-432) as shown by the XRD patterns (Fig. 1). No other crystalline phase was detected. The IR spectra of the samples (Fig. 2) exhibited intense bands characteristic of hydroxyapatite with the ν_2 (473 cm^{-1}), ν_4 (560 and 602 cm^{-1}), ν_1 (960 cm^{-1}) and ν_3 (1015 – 1030 and 1085 cm^{-1}) modes of PO_4^{3-}, as well as the librational (ν_L: 629 cm^{-1}) and stretching (ν_S: 3572 cm^{-1}) modes of the hydroxyl groups. Depending on the composition, other specific bands are noticeable. Spectra of particles synthesized in the presence of carbonates ions (*i.e.* CHA and CSiHA) exhibited bands, in the range 650-900 cm^{-1} and 1350-1600 cm^{-1}, characteristic of the incorporation of carbonate in HA structure (Lafon et al. 2008). These bands were assigned either to carbonate vibrations in A site (*i.e.* substituting for hydroxyl groups) or B site (*i.e.* substituting for phosphate groups) of the apatite. Spectra of SiHA and CSiHA samples displayed specific bands or shoulders attributed to SiO_4 in HA structure at 505 cm^{-1} (ν_2), 525 cm^{-1} (ν_4), 752 cm^{-1} (ν_1) and 891 cm^{-1} (ν_3) and 925 cm^{-1} (Si-OH) (Marchat et al. 2013). The presence of carbon and silicon in the samples was confirmed by elemental analysis (Table 1). As expected, the amount of carbon in CHA and CSiHA were similar, 1.2 and 1.3 wt. % respectively, as well as the amount of silicon in SiHA and CSiHA, 1.3 and 1.2 wt. % respectively. No traces of silicon was detected in HA and CHA samples. Traces of carbon measured in HA and SiHA were due to adsorbed carbon dioxide. After thermal treatment, the particles exhibited round shape morphologies (Fig. 3) with specific surface areas ranging from 14.5 to 21.6 m^2/g (Table 1). Whatever the chemistry, the sample displayed similar monodisperse particle size distribution in the 0.8 – 10.0 µm range (Fig. 4).

3.2. *In vitro* cellular response

3.2.1. Cellular morphology

Cells incubated for 24 h with particles have been observed after MGG staining. Representative optic microscopy images for the highest dose of particles are presented in Fig. 5. Cells with a lysed membrane and condensed nucleus were dead cells. They were identified in a same amount on the control as on the cells incubated with particles. Whatever the particle chemistry is, macrophages morphology after exposure to particles was similar to that of control cell. Images showed that particles were preferentially located in the cytoplasm periphery of the cells, close to the membrane surface. No clear evidence of the presence of vesicle was noticed.

3.2.2. Cell membrane integrity

Extracellular LDH directly correlates with the rate of cell membrane damage, since this enzyme is physiologically present in the cytoplasm. After incubation of the cells with the particles, the release of LDH was similar to that measured for the negative control (cells alone, Fig. 6). Moreover, no significant dose-response relationship was observed.

3.2.3. Pro-inflammatory response

All the particles exhibited significantly higher TNF-α production than the negative control (Fig. 7). At concentrations of 15 and 30 µg/mL, the particles induced similar pro-inflammatory responses. From 30 µg/mL, levels of TNF-α released in media significantly increased with the concentration of particles to reach around 850 pg/mL for a particle dose of 120 µg/mL, whatever the chemistry is.

3.2.4. Oxidative stress

The oxidative stress was determined by the ROS production. For a given time of exposure, levels of ROS were similar for all the particles chemistries and were twice higher at 24 h than at 90 min (Fig. 8). However, values were significantly lower than for the positive control (cells incubated with 1 mM of H_2O_2), whatever the experimental conditions (*i.e.* chemistry or particle dose) are.

4. Discussion

Particles of carbon- and/or silicon-substituted HA were prepared by adjusting a wet precipitation method conventionally used to synthesize substituted calcium phosphate powders (Marchat et al. 2013; Raynaud et al. 2002). Depending on their chemistry, the particles were heat treated at a specific temperature and under a specific atmosphere (Table 1). The XRD data showed that after thermal treatment, all the particles were monophasic. The CO_2 atmosphere used during the heat-treatment of carbon containing samples (*i.e.* CHA and CSiHA) allowed to maintain carbonate ions in the apatite lattice and to avoid phase decomposition (Boyer et al.

2013; Lafon et al. 2003). FTIR spectra of CHA and CSiHA revealed that carbonate substitution occurred on both phosphate and hydroxyl sites. As a consequence, intensities of hydroxyl groups for these samples logically decreased as compared to HA sample. In a same way, for SiHA sample, the decrease of intensity of the band for OH group was attributed to the creation of OH vacancies resulting from the incorporation of SiO_4 into HA structure (Marchat et al. 2013). Therefore, monophasic particles of stoichiometric and carbon and/or silicon substituted HA were produced and used for further biological experiments.

Shanbhag et al. (1994) proved that, additionally to chemistry, macrophages were sensitive to the surface developed by the particles present in the cell culture. In the present study, weight concentrations of spherical particles ranging from 15 to 120 µg/mL were used. As their specific surface area were in a same order of magnitude (Table 1), comparison between the different chemistries was possible. Moreover, particle sizes were in the range of the micron with a D50 around 2 µm. This size range was consistent with the size of particulate debris observed in *in vivo* studies from retrieved tissues (Benhayoune et al. 2000; Hing et al. 2007; Lu et al. 2004). The studied particles were in a clinically relevant range. Although it has been noted that particles were released from CaP based materials *in vivo*, no quantitative information on the particle number was reported in the above mentioned studies. Thus, it is difficult to address a direct correspondence between *in vivo* and *in vitro* studies. However, the particle concentrations used were comparable to the concentrations used in similar *in vitro* experiments (Lange et al. 2009; Pioletti et al. 2000; Zhang et al. 2012) and covered two orders of magnitude.

After implantation of a bone substitute, since a biomaterial is considered as a foreign body, the natural host response leads to the recruitment from the blood of monocytes which become macrophages (Anderson et al. 2008). Thus, the present biological evaluation was performed on macrophages that are, moreover, the major cells responsible for mediating the pro-inflammatory response to implant debris (Ingham et al. 2005). RAW 264.7 cell lines were selected due to their active role in an inflammatory response model and their activations and functions have been well established (Salitsky 1983). Data presented here revealed an absence of ROS generation by the macrophage, irrespective of the chemistry of the particles. The release of LDH was similar to that of the negative control, revealing no cytotoxicity. These results were consistent with the microscopic observations (Fig. 5) which revealed that, even for high dose of particles, cells presented morphology comparable to that of control cells.

The results also showed that substituted hydroxyapatite particles can trigger the production of the TNF-α cytokine by macrophage RAW 264.7. The inflammatory effect was dose-dependent, but no influence of SiO_4 and/or CO_3 substitution into HA was noticed. So, the chemistry of the studied particles did not induce changes in

TNF-α production. Lange et al. (2009) came to the same conclusion after studying HA and β-TCP particles of the same size incubated with human peripheral blood mononuclear cells: the particles elicited similar production of proinflammatory cytokines (TNF-α, IL-β and IL-8). However, the chemistry of CaP based materials highly influenced their dissolution behavior and, as a consequence, their ability to heal a bone defect. Indeed, an *in vivo* study, performed in a standard rabbit defect model, has shown that the poor performance of β-TCP biomaterials can be assigned to its high solubility that induced an early loss of integrity of the implant and of the bone apposition along with a proinflammatory response provoked by the release of particulate debris (Hing et al. 2007). This immunogenic response would be a consequence of the presence of high amount of β-TCP particles. This statement is supported *in vitro* by Zhang et al. (2012) who reported a 3-fold increase of the amount of TNF-α release by osteocytes-like cells when the concentration of β-TCP particles increases from 100 to 1000 µg/mL. Besides, TNF-α produced by macrophages may stimulate the expression of RANKL (Receptor Activator of Nuclear factor Kappa-B Ligand) and M-CSF (Macrophage Colony Stimulating Factor), together involved in the differentiation of osteoclast precursors into mature osteoclasts that resorb bone (Ingham et al. 2005). So, it clearly appears that, to efficiently heal a bone defect, the generation of particulate debris from the bioceramics must be restricted. It implies to adjust the degradation behavior of the current CaP materials in order to reach an intermediate behavior between that of HA and β-TCP, while having a material that at least, supports or even favors the bone apposition. These are the expected characteristics of CSiHA composition that contains carbonate (to control the rate of resorption and dissolution) and silicate (supposed to increase the early bone apposition) in substitution into HA. As the pro-inflammatory response is particle dose-dependent, further studies to characterize the degradation of CSiHA ceramics *in vivo* and *in vitro* are under progress and will be interpreted in the light of the present data. A complementary way to adjust the degradation behavior of CaP bone substitutes, especially for the challenging field of large bone defect reconstruction, would be to control their manufacturing process (*i.e.* shaping and sintering) in order to maintain the integrity of the bioceramic and to avoid a premature *in vivo* degradation. The recent advances in additive manufacturing technics coupled to computational models give opportunities to develop new designs of implants with complex architecture allowing maximizing the ratio between mechanical strength and degradation rate (Heljak et al. 2012).

5. **Conclusion**

In summary, micron sized particles composed of carbon- and/or silicon-substituted hydroxyapatite exhibited no *in vitro* toxicity for macrophages RAW 264.7. An equivalent dose-dependent pro-inflammatory response was

observed whatever the ionic substitution (CO_3 substitution for PO_4 and OH; SiO_4 substitution for PO_4 or CO_3 and SiO_4 co-substitution) is. These results provide evidence that for these compositions, between the chemistry and the particles concentration, the *in vitro* immunogenic response was mainly due to the latter. This conclusion should now be confirmed by *in vivo* experiments. Moreover, as the cytokine released by macrophage can alter the bone remodeling process, accurate evaluation of the degradation of these CaP bone substitutes must be performed to confirm their performance.

Conflict of Interest: The authors declare that they have no conflict of interest.

References

J.M. Anderson, A. Rodriguez, D.T. Chang. Semin Immunol 20, 86 (2008)

L.T. Bang, B.D. Long, R. Othman. The Scientific World Journal 2014, 9 (2014)

J. Barralet, M. Akao, H. Aoki, H. Aoki. J Biomed Mater Res 49, 176 (2000)

H. Benhayoune, E. Jallot, P. Laquerriere, G. Balossier, P. Bonhomme, P. Frayssinet. Biomaterials 21, 235 (2000)

G. Bouet, D. Marchat, M. Cruel, L. Malaval, L. Vico. Tissue engineering Part B, Reviews 21, 133 (2015)

A. Boyer, D. Marchat, D. Bernache-Assollant. Key Eng Mat 529-530, 100 (2013)

V. Campana, G. Milano, E. Pagano, M. Barba, C. Cicione, G. Salonna, W. Lattanzi, G. Logroscino. J Mater Sci-Mater M 25, 2445 (2014)

E.M. Carlisle. Science 167, 279 (1970)

E.M. Carlisle. Science 178, 619 (1972)

J.M. Curran, J.A. Gallagher, J.A. Hunt. Biomaterials 26, 5313 (2005)

R. Detsch, H. Mayr, G. Ziegler. Acta Biomater 4, 139 (2008)

S.V. Dorozhkin, M. Epple. Angew Chem Int Edit 41, 3130 (2002)

M.K. Heljak, W. Święszkowski, C.X.F. Lam, D.W. Hutmacher, K.J. Kurzydłowski. International Journal for Numerical Methods in Biomedical Engineering 28, 789 (2012)

K.A. Hing, L.F. Wilson, T. Buckland. The spine journal : official journal of the North American Spine Society 7, 475 (2007)

E. Ingham, J. Fisher. Biomaterials 26, 1271 (2005)

R. Jugdaohsingh. The journal of nutrition, health & aging 11, 99 (2007)

J.P. Lafon, E. Champion, D. Bernache-Assollant, R. Gibert, A.M. Danna. J Therm Anal Calorim 72, 1127 (2003)

J.P. Lafon, E. Champion, D. Bernache-Assollant. J Eur Ceram Soc 28, 139 (2008)

E. Landi, G. Celotti, G. Logroscino, A. Tampieri. J Eur Ceram Soc 23, 2931 (2003)

E. Landi, J. Uggeri, S. Sprio, A. Tampieri, S. Guizzardi. J Biomed Mater Res A 94A, 59 (2010)

T. Lange, A.F. Schilling, F. Peters, F. Haag, M.M. Morlock, J.M. Rueger, M. Amling. Biomaterials 30, 5312 (2009)

T. Lange, A.F. Schilling, F. Peters, J. Mujas, D. Wicklein, M. Amling. Biomaterials 32, 4067 (2011)

P. Laquerriere, A. Grandjean-Laquerriere, E. Jallot, G. Balossier, P. Frayssinet, M. Guenounou. Biomaterials 24, 2739 (2003)

J. Lu, M.C. Blary, S. Vavasseur, M. Descamps, K. Anselme, P. Hardouin. J Mater Sci Mater Med 15, 361 (2004)

D. Marchat, M. Zymelka, C. Coelho, L. Gremillard, L. Joly-pottuz, F. Babonneau, C. Esnouf, J. Chevalier, D. Bernache-assollant. Acta Biomater 9, 6992 (2013)

J.T. Ninomiya, J.A. Struve, C.T. Stelloh, J.M. Toth, K.E. Crosby. Journal of orthopaedic research : official publication of the Orthopaedic Research Society 19, 621 (2001)

A. Oryan, S. Alidadi, A. Moshiri, N. Maffulli. J Orthop Surg Res 9, 18 (2014)

K.V. Pavankumar, K.; Rameshbabu, N.; Muthupandi V. Key Eng Mat 493-494, 739 (2011)

D.P. Pioletti, H. Takei, T. Lin, P. Van Landuyt, Q. Jun Ma, S. Yong Kwon, K.L. Paul Sung. Biomaterials 21, (2000)

J.A. Planell, M. Navarro, in Bone Repair Biomaterials, ed. By J.A. Planell, S.M. Best, D. Lacroix, A. Merolli (Woodhead Publishing, 2009), pp. 3-24

A. Porter, N. Patel, R. Brooks, S. Best, N. Rushton, W. Bonfield. J Mater Sci Mater Med 16, 899 (2005)

S. Raynaud, E. Champion, D. Bernache-Assollant, P. Thomas. Biomaterials 23, 1065 (2002)

S. Raynaud, E. Champion, J.P. Lafon, D. Bernache-Assollant. Biomaterials 23, 1081 (2002)

D.M. Reffitt, N. Ogston, R. Jugdaohsingh, H.F.J. Cheung, B.A.J. Evans, R.P.H. Thompson, J.J. Powell, G.N. Hampson. Bone 32, 127 (2003)

C. Rey, B. Collins, T. Goehl, I.R. Dickson, M.J. Glimcher. Calcified Tissue Int 45, 157 (1989)

C. Rey, C. Combes, C. Drouet, M.J. Glimcher. Osteoporosis Int 20, 1013 (2009)

A. Salitsky. The Raw 264.7 Cell Line: A Valid Candidate for Studying Macrophage Activation: Hahnemann University, Department of Microbiology and Immunology; 1983.

A.S. Shanbhag, J.J. Jacobs, J. Black, J.O. Galante, T.T. Glant. J Biomed Mater Res 28, 81 (1994)

J.H. Shepherd, D.V. Shepherd, S.M. Best. J Mater Sci Mater Med 23, 2335 (2012)

G. Spence, N. Patel, R. Brooks, N. Rushton. J Biomed Mater Res A 90, 217 (2009)

G. Spence, N. Patel, R. Brooks, W. Bonfield, N. Rushton. J Biomed Mater Res A 92, 1292 (2010)

F. Velard, J. Braux, J. Amedee, P. Laquerriere. Acta Biomater 9, 4956 (2013)

Y. Zhang, M. Yan, A. Yu, H. Mao, J. Zhang. Toxicology 297, 57 (2012)

Table

Table 1. Thermal treatment applied to the calcium phosphate particles and their resulting physico-chemical characteristics

Particle chemistry	Thermal treatment	Carbon content / wt.%	Silicon content / wt.%	Specific surface area / $m^2.g^{-1}$
HA	800°C for 1 h under air	0.08 ± 0.01	0	20.6 ± 0.1
CHA	800°C for 2 h under CO_2	1.21 ± 0.02	0	14.5 ± 0.3
SiHA	890°C for 2 h under air	0.08 ± 0.01	1.3 ± 0.4	21.6 ± 0.2
CSiHA	870°C for 1 h under CO_2	1.33 ± 0.02	1.2 ± 0.4	20 ± 0.2

Figures

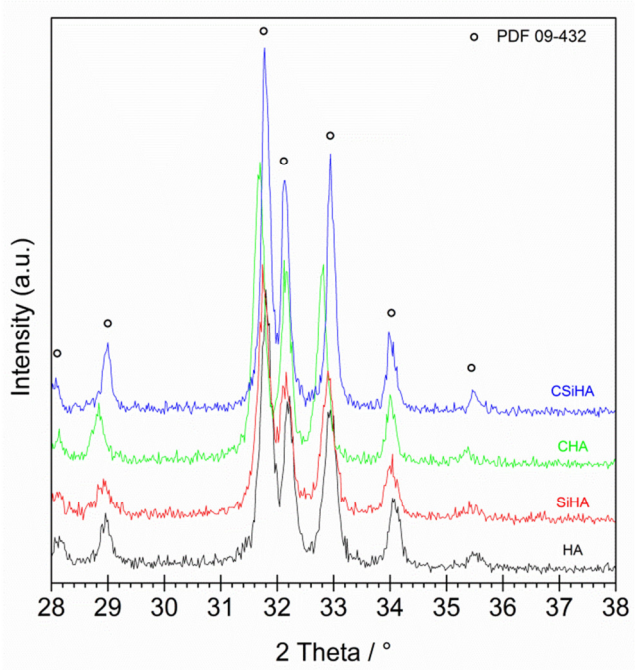

Fig. 1 X-Ray Diffraction patterns of calcium phosphate particles

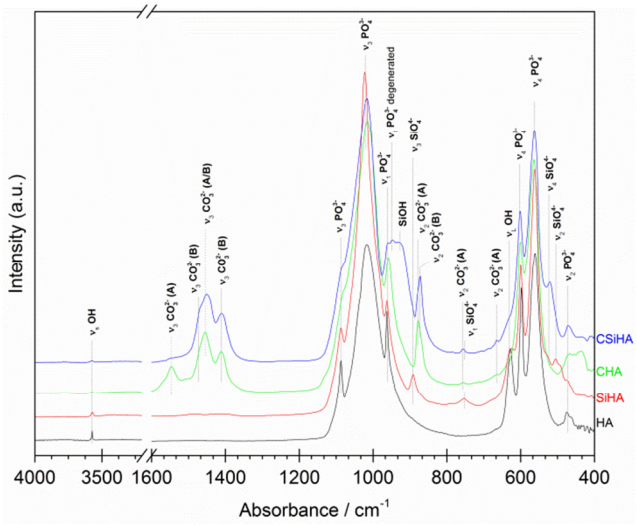

Fig. 2 FTIR spectra of calcium phosphate particles

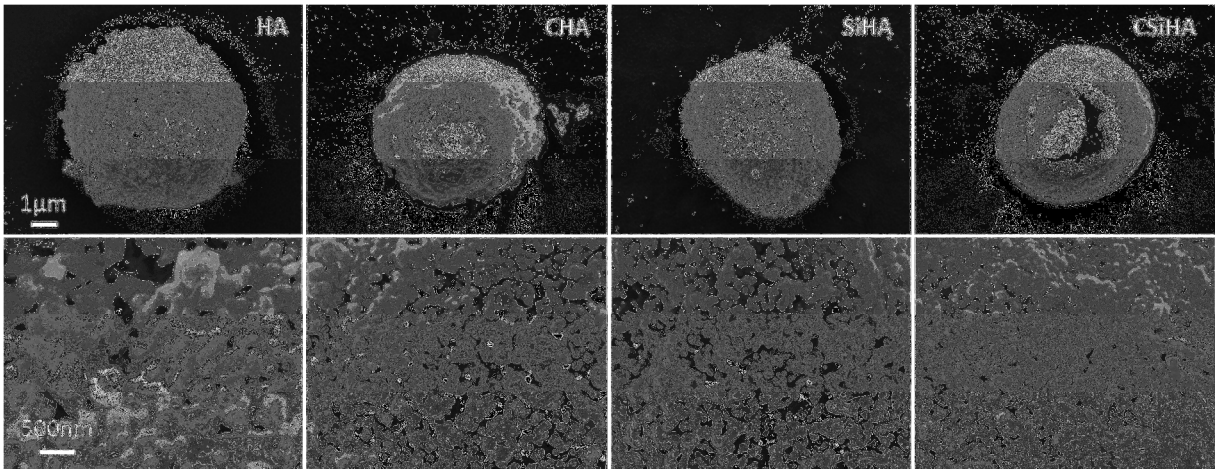

Fig. 3 Scanning Electron Microscopy images of calcium phosphate particles

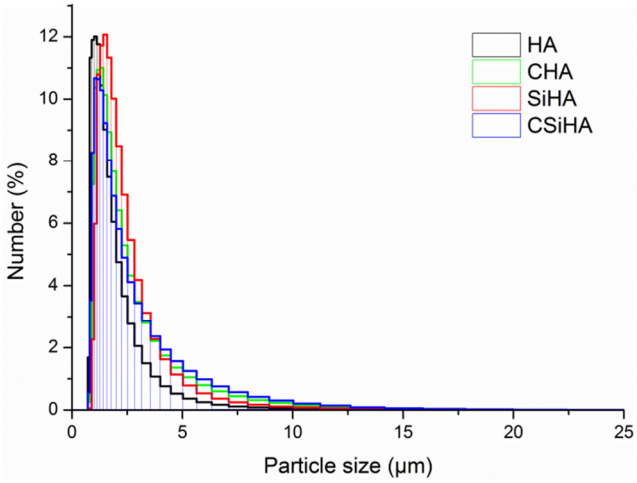

Fig. 4 Particle size distribution of the calcium phosphate suspensions

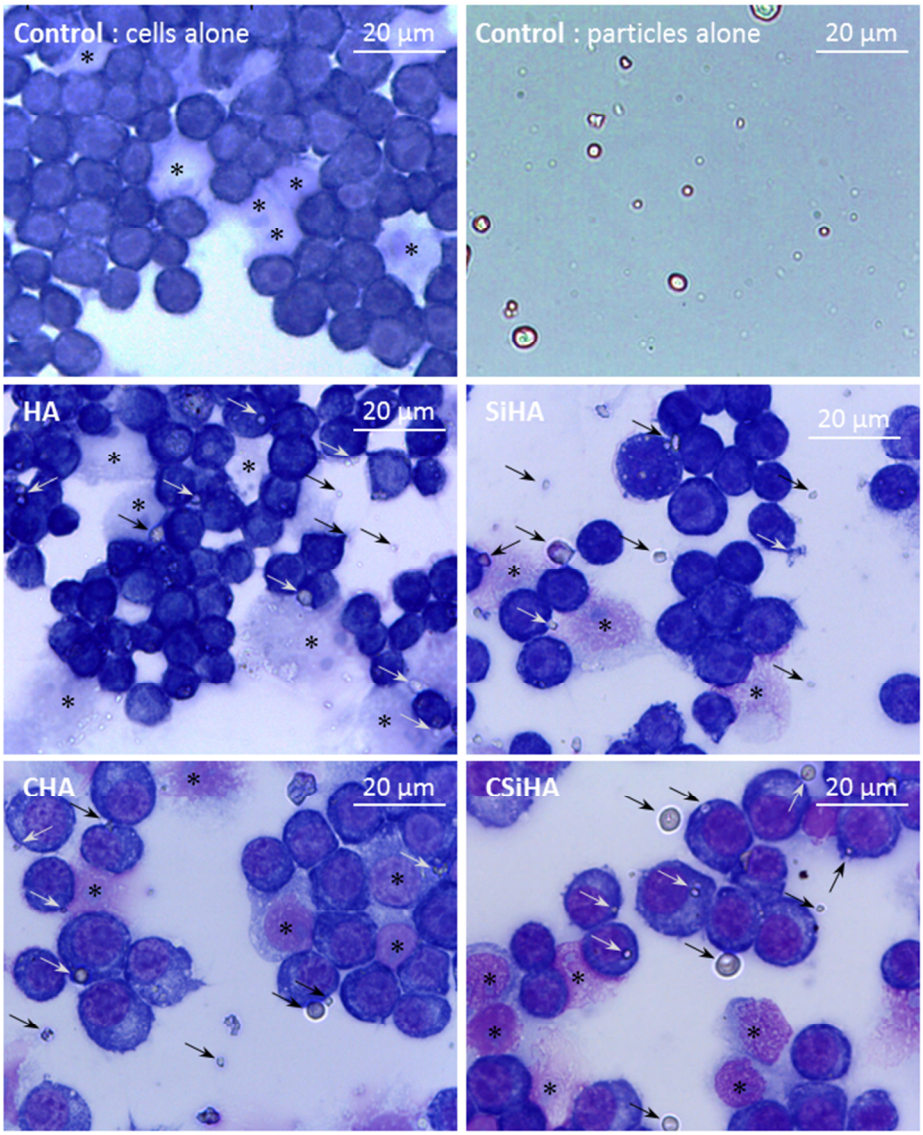

Fig. 5 Morphology of RAW 264.7 cells exposed for 24 h to 120 µg/mL of particles after May Grünwald Giemsa staining. Controls are macrophages incubated alone or particles of CSiHA at 120 µg/mL incubated alone; stars indicate dead cells and arrows indicate particles

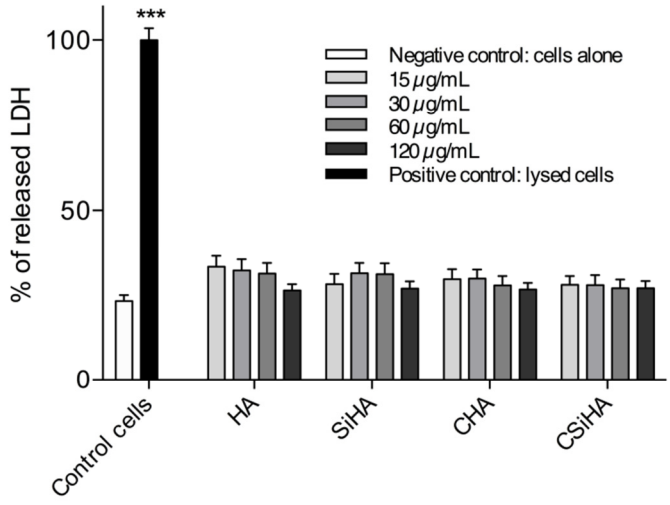

Fig. 6 Cytotoxicity determined by LDH release after 24 h exposure of RAW 264.7 cells with different dose of particles reported to that of total cellular LDH measured after the lysis of control cells (n = 3, *** $p < 0.001$)

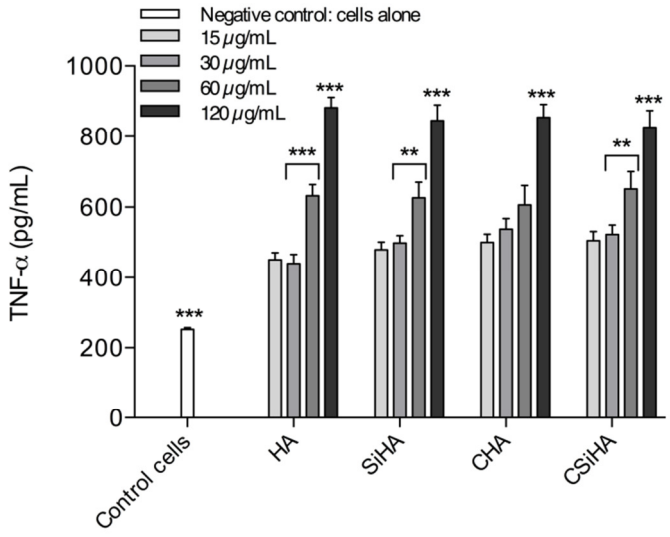

Fig. 7 Proinflammatory response determined by TNF-α production and measured after 24 h exposure of RAW 264.7 cells with different dose of particles (n = 3, *** $p < 0.001$, ** $p < 0.01$)

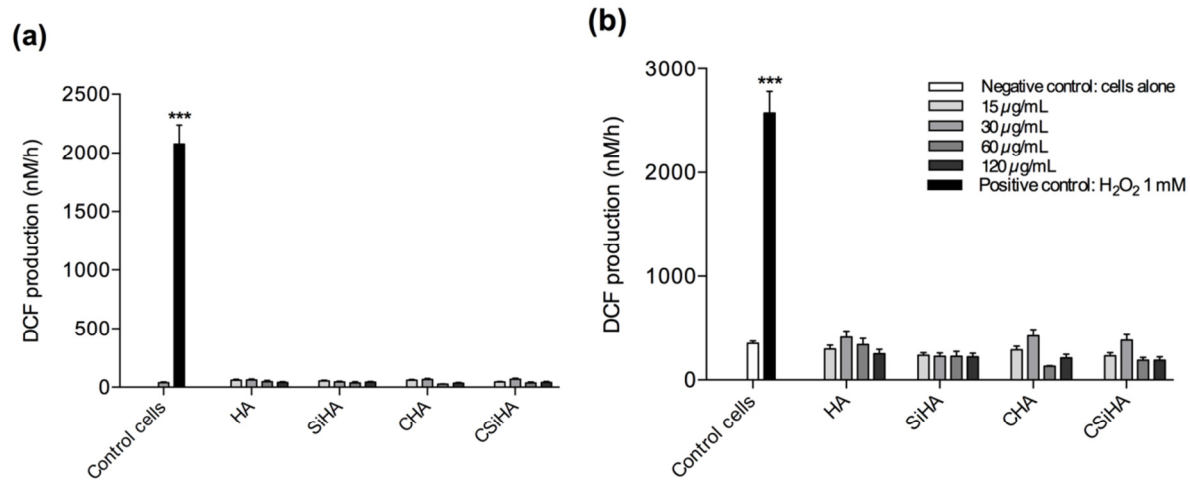

Fig. 8 Oxidative stress determined by ROS production after 90 min (a) and 24 h (b) exposure of RAW 264.7 cells with different dose of CaP particles (n = 3, *** $p < 0.001$). Results are expressed in nM/h of 2',7'-dichlorohidrofluorescein (DCF)